

# A New Fluorescent Probe for Selective Cd<sup>2+</sup> Detection and Cell Imaging

Wenxin Lin,<sup>\*,[a]</sup> Xiaochun Xie,<sup>[a]</sup> Yijia Wang,<sup>[a]</sup> and Jianjun Chen<sup>[a]</sup>

**Abstract.** A new highly selective fluorescent probe, (*E*)-4-(4-([2,2':6',2''-terpyridin]-4'-yl)styryl)-1-octadecylpyridin-1-ium bromide (ZC-F8), was designed and synthesized for cadmium detection and cell imaging. The fluorescence spectra of ZC-F8 exhibited its excellent response towards Cd<sup>2+</sup> via intramolecular charge transfer effect and

aggregation induced emission effect. The cell-imaging experiment was carried out to estimate the actual biological application of ZC-F8. The probe displayed ideal membrane permeable and labeled property for cadmium, indicating its promising application for metal ions detection and tracing in living cells.

## Introduction

Cadmium, as one of the important resources, has been widely used in many fields including electroplating, industry and agriculture. However, the toxic heavy metal Cd<sup>2+</sup> may cause acute or chronic poisoning resulting in cancers and other diseases.<sup>[1]</sup> Inevitably, rapid detection and efficient instantaneous monitoring of cadmium both in environment and biological systems are highly desirable and necessary.

Recently, fluorescent probes for detecting metal ions have been interested by researchers for their advantages, just like high sensitivity, briefness, and real-time detection.<sup>[2–5]</sup> So far, many fluorescent sensors are designed and synthesized for the Cd<sup>2+</sup> detection.<sup>[6–11]</sup> However, most of them bear the problem of selectivity due to other metal ions with similar chemical structures, such as Zn<sup>2+</sup>, which interfere the recognition. Generally, the photo-induced electron transfer (PET) effect, which adopts di-2-picolyamine (DPA) as ionophore for binding target ions, is employed for the design of Zn<sup>2+</sup> and Cd<sup>2+</sup> detection sensors. The fluorophore linking on the DPA unit can be quenched by the PET effect and the fluorescence is then recovered when specific metal ions coordinate with DPA to break the PET effect.<sup>[12–14]</sup> Therefore, the recognition capacity of sensors depend on the selective coordination of the ionophore with the target metal ions.<sup>[15,16]</sup> Nevertheless, the deficiency of selectivity may present on some metal pairs due to species with similar binding ability leading to the interruption by each other. In general, this phenomenon not only appears in Zn<sup>2+</sup>/Cd<sup>2+</sup>, but also in K<sup>+</sup>/Na<sup>+</sup>, Ag<sup>+</sup>/Hg<sup>2+</sup> and Ca<sup>2+</sup>/Mg<sup>2+</sup> pairs.

Till now, the development of sensors for tracing cadmium in cells with high sensitivity and selectivity still remains challenging. Jiang et al. introduced the carbonyl group to a fluorescent molecule for improving the sensing efficiency between Zn<sup>2+</sup> and Cd<sup>2+</sup>.<sup>[17,18]</sup> Lin et al. have reported a sensor, which

exhibits differential response to Zn<sup>2+</sup> and Cd<sup>2+</sup>.<sup>[19]</sup> Ng et al. synthesized two fluorescent probes for distinct detection of Zn<sup>2+</sup> and Cd<sup>2+</sup> by BODIPY.<sup>[20]</sup> Besides, Das et al. obtained a fluorescent probe to detect three metal ions (Zn<sup>2+</sup>, Cd<sup>2+</sup> and Pb<sup>2+</sup>) and to distinguish one from another via chelation-enhanced fluorescence mechanism, resulting from the chelation induced the internal charge transfer process.<sup>[21]</sup> However, most of the probes are not applicable in the cell imaging for the sake of their high cytotoxicity.

The new sensitive and selective fluorescent probes for sensing metal ions has attracted our attentions for several years.<sup>[22–25]</sup> Especially, the fluorescent sensors recognize Cd<sup>2+</sup> from Zn<sup>2+</sup> via the intramolecular charge transfer (ICT) effect.<sup>[26–28]</sup> However, some defects remain in these probes restricting their application in the biological field. The poor solubility of ZC-F1 limits its biological application, and the broadband emission range of ZC-F2 causes serious signal overlay in Zn<sup>2+</sup>/Cd<sup>2+</sup> pair. Therefore, the synthesis of satisfactory fluorescent probe is desired to improve its bioapplication.

In this work, a new fluorescent probe (*E*)-4-(4-([2,2':6',2''-terpyridin]-4'-yl)styryl)-1-octadecylpyridin-1-ium bromide (ZC-F8, Figure 1) is designed and synthesized to solve the problems mentioned above. Terpyridine, a good receptor for Cd<sup>2+</sup> and Zn<sup>2+</sup>, is conjugated with pyridinium by the styryl group, establishing a conjugated system in the molecule. Meantime, the pyridinium group can improve solubility to advance the hydrophilia of the fluorescent sensor. Besides, an

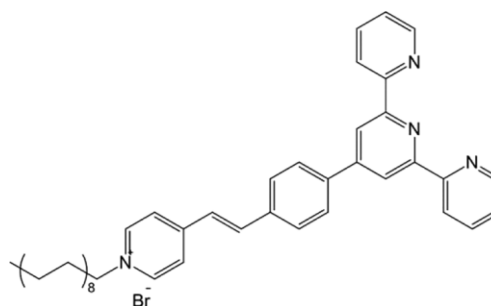


**Figure 1.** Structure of probe ZC-F8.

\* Dr. W. Lin

E-Mail: linwx@zstu.edu.cn

[a] College of Materials and Textiles  
Zhejiang Sci-Tech University  
Hangzhou 310018, P. R. China

alkane with sixteen carbon atoms is introduced into the molecule, which is found to be efficient for labeling cell membrane. It is supposed that the probe can localize on the surface of the cell membrane when it is injected in the living cells. After combination with  $\text{Cd}^{2+}$ , this probe may leave the membrane surface with different fluorescent emission colors, due to the change on molecular electrical properties. Thus, a probe for labeling  $\text{Cd}^{2+}$  in cells can be expected.

## Results and Discussion

As shown in Scheme 1, the molecule ZC-F8 was synthesized from commercially available chemicals through several steps. The detailed synthetic route and the structure characterization of ZC-F8 were described in the Experimental Section.

To check the aggregation induced emission (AIE) effect of obtained ZC-F8, the fluorescence spectra of probe were investigated in DMSO/ $\text{H}_2\text{O}$  system (Figure 2). Generally, aggregates would form when a suitable amount of nonsolvent was added, which was a common method to estimate AIE behavior in solvent/nonsolvent mixtures. In DMSO solution, ZC-F8 emitted weak fluorescence. The active intramolecular rotations of multiple pyridinium rings exhausted the excited state energy, resulting in fluorescence quenching. Finally the fluorescence intensity decreased with the water fraction ( $f_w$ , by volume %) increased, because of the twisted intramolecular charge-transfer process of probe with *D-A* structure. When  $f_w$  was over 80%, the probe molecules aggregated and the intramolecular rotations were limited, and the excited states decayed to the corresponding ground states via strong fluorescent emission. Therefore, ZC-F8 emitted bright fluorescence and the emission peak red shifted. The fluorescence was intensified with the incremental addition of water, indicating the AIE effect of ZC-F8.

The fluorescence spectra of ZC-F8 and its response towards  $\text{Zn}^{2+}$  and  $\text{Cd}^{2+}$  were taken out in solution (water/DMSO = 99:1) at  $1\ \mu\text{M}$  (Figure 3). Weak fluorescent emissions were gained before and after the titration of either  $\text{Zn}^{2+}$  or  $\text{Cd}^{2+}$  due to the high polarity of water.<sup>[29–31]</sup> Nevertheless, bright blue-green fluorescent emission could be observed when the probe

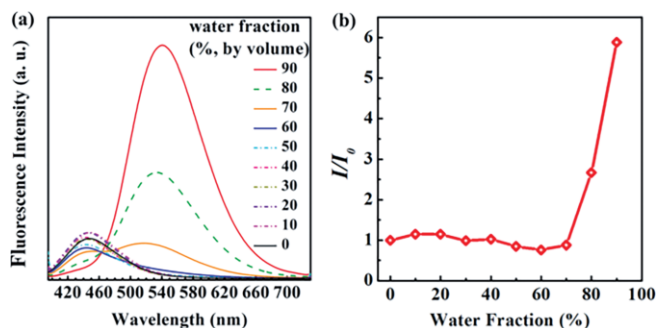


**Figure 2.** (a) Fluorescence (FL) spectra of ZC-F8 ( $10\ \mu\text{M}$ ) in the DMSO/ $\text{H}_2\text{O}$  system with different water fraction ( $f_w$ ) excited at  $375\ \text{nm}$ . (b) Plot of the changes of the peak FL intensity of ZC-F8 with variation of  $f_w$ . ( $I_0$  = the peak FL intensity of ZC-F8 when  $f_w$  is zero.)

was dried on the silicon sheet. This phenomenon could be ascribed to the AIE property of ZC-F8. The probe molecules dissipated excited state energy by motions in solution, while their motions were limited when they are solid state resulting in fluorescent emission to dissipate the excited state energy.

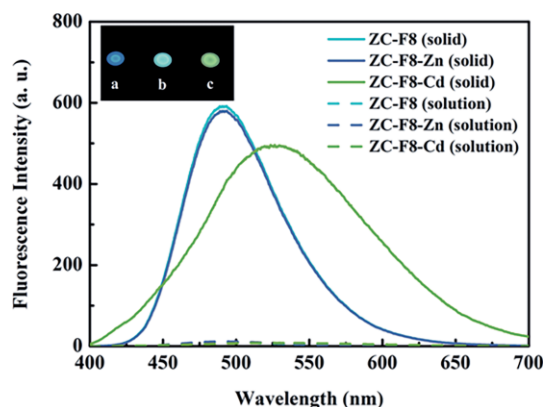
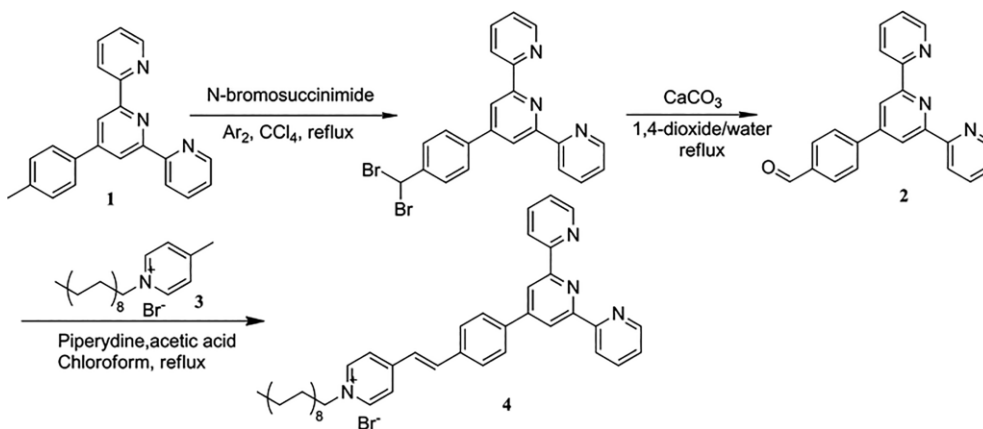


**Figure 3.** Fluorescence spectra of ZC-F8 ( $1\ \mu\text{M}$ ) excited at  $375\ \text{nm}$  upon addition of  $\text{Zn}^{2+}$  (0 and  $1.2\ \mu\text{M}$ ) or  $\text{Cd}^{2+}$  (0 and  $1.2\ \mu\text{M}$ ). Insets: the luminescence photograph of ZC-F8 before (b) and after addition of  $\text{Zn}^{2+}$  (a) and  $\text{Cd}^{2+}$  (c).



**Scheme 1.** Synthesis of probe ZC-F8.

ZC-F8 exhibited a broadband emission band peaked at 480 nm, which might be resulted from the strong electronic push-pull effect, indicating the strong ICT effect in the molecule. The initial fluorescence band of ZC-F8 disappeared and a new emission peak at 530 nm was observed after titrated with  $\text{Cd}^{2+}$ . Meanwhile, the fluorescence spectrum of ZC-F8 had no obvious variation after addition of  $\text{Zn}^{2+}$ , which was known as one of the most important interference of  $\text{Cd}^{2+}$ , revealing that the probe ZC-F8 could be applied for distinguishing  $\text{Cd}^{2+}$  from  $\text{Zn}^{2+}$ . The selective fluorescence responses might be ascribed to the combination of sensor ZC-F8 and the metal ions.<sup>[21,32]</sup> The different sized, electronic behavior, and charge density of metal ions resulting in the distinct ICT effect, leading to the change of emission colors. The probe ZC-F8 exhibited differential detection of  $\text{Zn}^{2+}/\text{Cd}^{2+}$ .

To further determine the selectivity of ZC-F8 in the practical environment, some other metal ions (such as  $\text{Hg}^{2+}$ ,  $\text{Ag}^+$ ,  $\text{Fe}^{3+}$ ,  $\text{Na}^+$ ,  $\text{Ca}^{2+}$ ,  $\text{Pb}^{2+}$ ,  $\text{Al}^{3+}$ ,  $\text{Co}^{2+}$ ,  $\text{Cu}^{2+}$ , and  $\text{K}^+$ ) were also utilized to assess their interference on the selectivity of ZC-F8 for detecting  $\text{Cd}^{2+}$ . As shown in Figure 4, the introduction of main group metal ions exhibited no influence on the fluorescence intensity when ZC-F8 was coordinated with  $\text{Cd}^{2+}$ , whereas  $\text{Fe}^{3+}$ ,  $\text{Co}^{2+}$ ,  $\text{Cu}^{2+}$ , and  $\text{Pb}^{2+}$  quenched the intensity in a minor degree. In addition,  $\text{Hg}^{2+}$  and its common interference  $\text{Ag}^+$  displayed no interruption, although Hg lied in the same group as Zn and Cd.

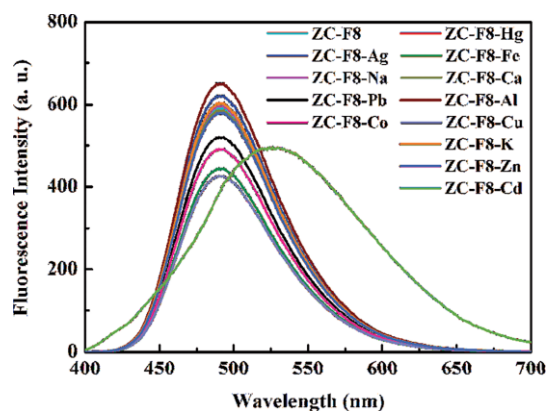


**Figure 4.** Fluorescence spectra of ZC-F8 (1  $\mu\text{M}$ ) dropped on silicon sheets before and after addition of  $\text{Cd}^{2+}$  and various interferences (5  $\mu\text{M}$  for  $\text{K}^+$ ,  $\text{Ca}^{2+}$ ,  $\text{Na}^+$  and  $\text{Al}^{3+}$  and 1.2  $\mu\text{M}$  for others) upon excitation at 395 nm.

Considering the excellent sensing properties for  $\text{Cd}^{2+}$  in vitro, the investigation of whether ZC-F8 could recognize  $\text{Cd}^{2+}$  in living cells was taken out by labeling HeLa cells. As controlled, the cells were cultured with ZC-F8 (10  $\mu\text{M}$ ) for 30 min, which emitted strong fluorescence on the cell membrane in the range of 460–500 nm. Other cells were treated with ZC-F8 (10  $\mu\text{M}$ ) for 15 min, and then were cultured in DMEM solution ( $\text{CdCl}_2$ , 5  $\mu\text{M}$ ) for another 15 min. After that, the cells were rinsed to remove excess  $\text{CdCl}_2$  and the fluorescence (510–600 nm) was observed obviously in cell nucleus (Figure 5). The bright-field images (Figure 5a and d) showed the cells were viable in the imaging experiments, indicating there was no effect of treatment with ZC-F8 and  $\text{Cd}^{2+}$ . As

shown in Figure 5b and e, the fluorescent probe ZC-F8 gathered in cell membrane due to the alkane part of probe molecule. The fluorescent molecules passed through cell membrane and labeled  $\text{Cd}^{2+}$  in cell nucleus after the addition of  $\text{Cd}^{2+}$ . These remarkable alterations indicated that ZC-F8 could pass through the cell membrane and detect  $\text{Cd}^{2+}$  in living cells. It could be used as a helpful probe for observing the distribution of  $\text{Cd}^{2+}$  in living cells and investigating the influence of cadmium on the cells.

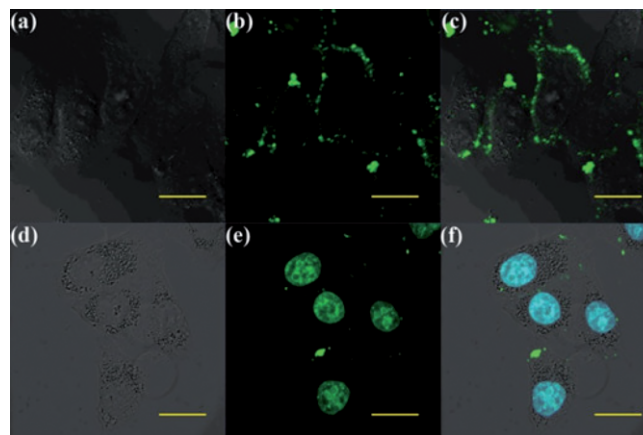


**Figure 5.** Fluorescence images of HeLa cells cultured with ZC-F8 (10  $\mu\text{M}$ ) and  $\text{CdCl}_2$  [0  $\mu\text{M}$  (a–c); 5  $\mu\text{M}$  (d–f)]. Panels (a) and (d) show differential interference contrast (DIC) images, Panels (b) and (e) display the corresponding confocal fluorescence images collected at 460–500 nm and 510–600 nm, respectively. Panel (c) is the overlap of (a) and (b). Panel (f) is the image of HeLa cells cultured with both ZC-F8 and Hoechst 33342. The wavelength for excitation is 405 nm. The scale bar is 10  $\mu\text{m}$ .

## Conclusions

A new highly selective fluorescent probe for  $\text{Cd}^{2+}$  detection in environment and living cells was obtained. This probe shows potential usage in the detection of  $\text{Cd}^{2+}$ . By utilizing metal ions as a part of the conjugated system, the sensor can response to  $\text{Cd}^{2+}$  at aggregated state via ICT and AIE effects. In addition, the cell-imaging experiment shows the desired cell membrane permeable and satisfactory tracing property for  $\text{Cd}^{2+}$  of ZC-F8. It is an interesting probe capable of detecting and labeling  $\text{Cd}^{2+}$  in cell, indicating the design of such molecules can be applied in future researches on tracing metal ions in living cells.

## Experimental Section

**General:** In this work, all the chemical reagents were gained from commercial source and used without further purification.  $^1\text{H}$  NMR spectra were performed with a Bruker Avance DMX500 spectrometer using tetramethylsilane (TMS) as an internal standard. Elemental analysis was carried out with a Thermo Finnigan Flash EA1112 microelemental analyzer. Fluorescence spectra and excitation spectra were taken out with a Hitachi F4600 fluorescence spectrophotometer. Fluorescence images were gained with an Olympus FV-1000 confocal laser scanning microscope.

**4'-(*p*-Methylphenyl)-2,2':6',2''-terpyridine (1):** NaOH (0.22 g, 5.4 mmol) and  $\text{NH}_4\text{OH}$  (30 mL) were introduced into a methanol solu-

tion (120 mL) of 4-methylbenzaldehyde (0.65 g, 5.4 mmol) and 2-acetylpyridine (1.3 g, 10.8 mmol). The resulting solution was refluxed for 12 h, and the precipitate emerged after it was cooled down to room temperature. Afterwards, the precipitate was filtered, affording a white powder of **1** (1.05 g, 40%). <sup>1</sup>H NMR (500 MHz, CDCl<sub>3</sub>): δ = 2.34 (s, 3 H, CH<sub>3</sub>), 7.44 (s, 2 H, ArH), 7.67 (d, 2 H, *J* = 2 Hz, ArH), 7.85 (d, 2 H, *J* = 8 Hz, ArH), 7.97 (s, 2 H, ArH), 8.74 (d, 2 H, *J* = 7 Hz, ArH), 8.78 (t, 4 H, *J* = 12 Hz, ArH) ppm. C<sub>22</sub>H<sub>17</sub>N<sub>3</sub>: calcd. C 81.71; N 12.99; H 5.30%; found: C 81.59; N 13.10; H 5.31%.

**4-([2,2':6',2''-Terpyridin]-4'-yl)benzaldehyde (2):** In an atmosphere of argon, the CCl<sub>4</sub> solution (20 mL) containing reactant **1** (1.0 g, 3.1 mmol) was stirred for 15 min. Afterwards, the solution was refluxed for 24 h after the introduction of benzoyl peroxide (0.049 g, 0.2 mmol) and *N*-bromosuccinamide (1.23 g, 6.2 mmol). The resulting mixture was cooled to room temperature and evaporated to obtain a yellow solid. The yellow solid was added into a mixture solution (CaCO<sub>3</sub>, 1.0 g; 1,4-dioxane, 40 mL; water, 10 mL) and was refluxed for another 24 h. Finally, the resulting solution was evaporated and purified by chromatography, using EtOAc and petroleum (1:2) as eluent, to get pale solid **2** (0.50 g, 48%). <sup>1</sup>H NMR (500 MHz, CDCl<sub>3</sub>): δ = 7.35 (m, 2 H, *J* = 5 Hz, ArH), 7.87 (m, 2 H, ArH), 8.01 (m, 4 H, *J* = 8 Hz, ArH), 8.66 (d, 2 H, *J* = 8 Hz, ArH), 8.72 (t, 4 H, ArH), 10.8 (s, 1 H, CHO) ppm. C<sub>22</sub>H<sub>15</sub>N<sub>3</sub>O: calcd. C 78.32; N, 12.46; H, 4.48%; found: C 78.39; N, 12.50; H, 4.41%.

**(E)-4-(4-([2,2':6',2''-Terpyridin]-4'-yl)styryl)-1-octadecylpyridin-1-ium bromide (ZC-F8):** The reactant **2** (1.34 g, 4 mmol) and 4-methyl-1-octadecylpyridin-1-ium bromide (**3**) (2.55 g, 6 mmol) were dissolved in CHCl<sub>3</sub> (20 mL). Afterwards, piperidine (0.1 mL) was added and the mixture was refluxed for 24 h. The organic phase, which was extracted from the resulting mixtures, was dried with MgSO<sub>4</sub>. The solvent was removed and the desired product **ZC-F8** (0.55 g, 19%) was purified by chromatography with mixed solution (CH<sub>2</sub>Cl<sub>2</sub>:EtOAc, 20:1). <sup>1</sup>H NMR (500 MHz, CDCl<sub>3</sub>): δ = 1.03 (s, 3 H, CH<sub>2</sub>CH<sub>3</sub>), 1.55 (m, 30 H, CH<sub>2</sub>), 2.47 (m, 2 H, CH<sub>2</sub>), 4.66 (m, 2 H, CH<sub>2</sub>), 6.48 (s, 1 H, ArH), 6.65 (d, 1 H, ArH), 7.30 (m, 2 H, ArH), 7.43 (d, 1 H, *J* = 9 Hz, ArH), 7.78 (d, 2 H, CH=CH), 7.94 (m, 3 H, ArH), 8.02 (d, 2 H, ArH), 8.25 (d, 1 H, ArH), 8.59 (s, 1 H, ArH), 8.62 (d, 2 H, ArH), 8.73 (m, 4 H, ArH) ppm. C<sub>46</sub>H<sub>57</sub>BrN<sub>4</sub>: calcd. C 74.07; N, 7.51; H, 7.70%; found: C 74.52; N, 7.38; H, 7.57%.

**Cell Culture:** HeLa human cervical carcinoma cells were selected to incubate in Dulbecco's Modified Eagle's Medium (DMEM, Neuronbc) with 10% fetal bovine serum (FBS, sijinging), penicillin (100 units per mL, Boster) and streptomycin (100 μg·mL<sup>-1</sup>, Boster). Firstly, the cells were seeded on glass-bottomed dishes. After 48 h of incubation, the cultured medium was replaced with fresh DMEM without FBS. For imaging, the cells were cultured in DMSO stock solution containing ZC-F8 (10 μM) at 37 °C under 5% CO<sub>2</sub> for 15 min. Then, the cells were incubated in DMEM solution (containing 5 μM or 0 μM CdCl<sub>2</sub>) for another 15 min under the same condition. After that, the treated cells were rinsed 3 times with phosphate buffered saline (PBS, pH 7.2) and observed by the confocal laser scanning microscope.

## Acknowledgements

The authors gratefully acknowledge the financial support for this work from the National Natural Science Foundation of China (No. 51802283).

**Keywords:** Fluorescent probe; Selectivity; Imaging agents; Cadmium; Cd<sup>2+</sup> labeling; Cell nucleus

## References

- [1] G. F. Jiang, L. Xu, S. Z. Song, C. C. Zhu, Q. Wu, L. Zhang, *Toxicology* **2008**, *244*, 49–55.
- [2] F. X. Cheng, N. Tang, K. C. Miao, F. Wang, *Z. Anorg. Allg. Chem.* **2014**, *640*, 1816–1821.
- [3] L. Fang, L. Zhang, Z. Chen, C. Zhu, J. Liu, *J. Mater. Lett.* **2017**, *191*, 1–4.
- [4] T. M. Elmorsi, T. S. Aysha, M. B. Sheier, A. H. Bedair, *Z. Anorg. Allg. Chem.* **2017**, *643*, 811–818.
- [5] Z. Zhou, K. Shih, Y.-P. Cai, L. Szeto, W.-T. Wong, *Z. Anorg. Allg. Chem.* **2014**, *640*, 1494–1498.
- [6] M. Taki, M. Desaki, A. Ojida, S. Iyoshi, T. Hirayama, I. Hamachi, Y. Yamamoto, *J. Am. Chem. Soc.* **2008**, *130*, 12564–12565.
- [7] F. Duan, G. Liu, P. Liu, C. Fan, S. Pu, *Tetrahedron* **2016**, *72*, 3213–3220.
- [8] A. Sil, A. Maity, D. Giri, S. K. Patra, *Sensor Actuat. B, Chem.* **2016**, *226*, 403–411.
- [9] X. Ding, F. Zhang, Y. Bai, J. Zhao, X. Chen, M. Ge, W. Sun, *Tetrahedron Lett.* **2017**, *58*, 3868–3874.
- [10] R. Feng, Y. Hou, Z. Z. Wu, Y. Yang, F. M. Nie, *Z. Anorg. Allg. Chem.* **2015**, *641*, 1918–1925.
- [11] C. R. Johnson, J. D. Shrout, J. B. Fein, *Chem. Geol.* **2018**, *483*, 21–30.
- [12] S. Doose, H. Neuweiler, M. Sauer, *ChemPhysChem* **2009**, *10*, 1389–1398.
- [13] A. P. de Silva, H. Q. N. Gunaratne, T. Gunlaugsson, A. J. M. Huxley, C. P. McCoy, J. T. Rademacher, T. E. Rice, *Chem. Rev.* **1997**, *97*, 1515–1566.
- [14] J. S. Wu, W. M. Liu, J. C. Ge, H. Y. Zhang, P. F. Wang, *Chem. Soc. Rev.* **2011**, *40*, 3483–3495.
- [15] D. W. Domaille, E. L. Que, C. J. Chang, *Nat. Chem. Biol.* **2008**, *4*, 168–175.
- [16] K. Boonkitpatarakul, A. Smata, K. Kongnukool, S. Srisurichan, K. Chainok, M. Sukwattanasinitt, *J. Lumin.* **2018**, *198*, 59–67.
- [17] L. Xue, C. Liu, H. Jiang, *Org. Lett.* **2009**, *11*, 1655–1658.
- [18] L. Xue, Q. Liu, H. Jiang, *Org. Lett.* **2009**, *11*, 3454–3457.
- [19] J. L. Wang, W. Y. Lin, W. L. Li, *Chem. Eur. J.* **2012**, *18*, 13629–13632.
- [20] H. He, D. K. P. Ng, *Chem. Asian J.* **2013**, *8*, 1441–1446.
- [21] S. Samanta, B. K. Datta, M. Boral, A. Nandan, G. Das, *Analyst* **2016**, *141*, 4388–4393.
- [22] Y. Q. Tan, J. C. Yu, Y. J. Cui, Y. Yang, Z. Y. Wang, X. P. Hao, G. D. Qian, *Analyst* **2011**, *136*, 5283–5286.
- [23] Y. Q. Tan, J. C. Yu, J. K. Gao, Y. J. Cui, Z. Q. Wang, Y. Yang, G. D. Qian, *RSC Adv.* **2013**, *3*, 4872–4875.
- [24] Y. Q. Tan, J. C. Yu, J. K. Gao, Y. J. Cui, Y. Yang, G. D. Qian, *Dyes Pigm.* **2013**, *99*, 966–971.
- [25] Y. Q. Tan, Q. Zhang, J. C. Yu, X. Zhao, Y. P. Tian, Y. J. Cui, X. P. Hao, Y. Yang, G. D. Qian, *Dyes Pigm.* **2013**, *97*, 58–64.
- [26] Y. Q. Tan, J. K. Gao, J. C. Yu, Z. Q. Wang, Y. J. Cui, Y. Yang, G. D. Qian, *Dalton Trans.* **2013**, *42*, 11465–11470.
- [27] Q. Hu, Y. Q. Tan, M. Liu, J. C. Yu, Y. J. Cui, Y. Yang, *Dyes Pigm.* **2014**, *107*, 45–50.
- [28] Y. Q. Tan, M. Liu, J. K. Gao, J. C. Yu, Y. J. Cui, Y. Yang, G. D. Qian, *Dalton Trans.* **2014**, *43*, 8048–8053.
- [29] R. S. Mulliken, *J. Phys. Chem.* **1952**, *56*, 801–822.
- [30] R. S. Mulliken, *J. Am. Chem. Soc.* **1952**, *74*, 811–824.
- [31] A. Marini, A. Muñoz-Losa, A. Biancardi, B. Mennucci, *J. Phys. Chem. B* **2010**, *114*, 17128–17135.
- [32] Y. Hu, Q. Q. Li, H. Li, Q. N. Guo, Y. G. Lu, Z. Y. Li, *Dalton Trans.* **2010**, *39*, 11344–11352.

Received: October 18, 2018

Published Online: ■

W. Lin,\* X. Xie, Y. Wang, J. Chen ..... 1–6

A New Fluorescent Probe for Selective  $\text{Cd}^{2+}$  Detection and Cell Imaging

